Measles Metapopulation Dynamics: A Gravity Model for Epidemiological Coupling and Dynamics

Yingcun Xia,[1,*] Ottar N. Bjørnstad,[2,†] and Bryan T. Grenfell[3,‡]

1. Department of Statistics and Applied Probability, National University of Singapore, Singapore;
2. Departments of Entomology and Biology, Pennsylvania State University, University Park, Pennsylvania 16802;
3. Department of Zoology, University of Cambridge, Cambridge CB2 3EJ, United Kingdom

Submitted June 23, 2003; Accepted January 12, 2004; Electronically published July 8, 2004

Online enhancements: appendix, figures.

ABSTRACT: Infectious diseases provide a particularly clear illustration of the spatiotemporal underpinnings of consumer-resource dynamics. The paradigm is provided by extremely contagious, acute, immunizing childhood infections. Partially synchronized, unstable oscillations are punctuated by local extinctions. This, in turn, can result in spatial differentiation in the timing of epidemics and, depending on the nature of spatial contagion, may result in traveling waves. Measles epidemics are one of a few systems documented well enough to reveal all of these properties and how they are affected by spatiotemporal variations in population structure and demography. On the basis of a gravity coupling model and a time series susceptible-infected-recovered (TSIR) model for local dynamics, we propose a metapopulation model for regional measles dynamics. The model can capture all the major spatiotemporal properties in prevaccination epidemics of measles in England and Wales.

Keywords: gravity models, measles, SIR model, phase difference, TSIR model, wavelet.

Infectious diseases provide a particularly clear illustration of the spatiotemporal underpinnings of consumer-resource dynamics. The paradigm is provided by the locally unstable, oscillatory dynamics of extremely contagious, acute, immunizing childhood infections (Bartlett 1956, 1957; Schenzle 1984; Anderson and May 1991; Cliff et al. 1993; Grenfell et al. 2001). In particular, measles dynamics have sparked a long history of data analysis and modeling across a range of disciplines. Mathematical epidemiologists, drawn by the importance of the disease, have dissected most of the main features of measles transmission within local communities. From the point of view of the local dynamics, there are three interlocking issues. First, seasonality in transmission interacts with epidemic nonlinearities to shape the attractor of the dynamical system (Dietz 1976; Schenzle 1984; Bjørnstad et al. 2002). Second, host demography, particularly birthrates and immunization through vaccination, interacts with transmission to influence the disease dynamics (McLean and Anderson 1988; Finkenstädt et al. 1998; Earn et al. 2000; Finkenstädt and Grenfell 2000; Grenfell et al. 2002). Finally, the stochasticity inherent in the epidemic birth and death process (Bartlett 1956; Bailey 1975; Olsen and Schaffer 1990) can excite recurrent epidemics (Bartlett 1956; Dietz 1976; Schenzle 1984; Bjørnstad et al. 2002) but also cause local extinction in the troughs between epidemics (Bartlett 1956; Cliff et al. 1993; Grenfell and Harwood 1997). While measles dynamics are arguably specific to the dynamics of infectious childhood diseases, these main issues parallel the dynamics of many consumer-resource systems (Wilson and Hassell 1997; King and Schaffer 2001).

Local extinction of viral microparasites results when the local chain of transmission is broken (Grenfell and Harwood 1997). This tends to happen in small host populations, since an epidemic reduces the susceptible numbers and diminishes the force of infection to where demographic stochasticity leads to breaks in the chain of transmission. Fifty years ago, Bartlett (1956) recognized this in his epidemic taxonomy of measles, which divides dynamics into Type I behavior (endemic cycles in large cities), Type II dynamics in medium-sized communities (predictable epidemics but with local extinction during epidemic troughs), and Type III dynamics in small communities (irregular epidemics interspersed by prolonged periods of local disease extinction, so-called epidemic fade-outs). For humans and other social animals in which hosts are dis-

* E-mail: staxyc@stat.nus.edu.sg.

† E-mail: onb1@psu.edu.

‡ E-mail: btg11@cam.ac.uk.

Am. Nat. 2004. Vol. 164, pp. 267–281. 0003-0147/2004/16402-30242$15.00.

tributed in heterogeneous patches, there are two critical sides to transmission. The first is local transmission among individuals within "patches" (cities, towns, and villages). The second is transmission between patches. With this point of view, there is a clear conceptual link between ecological and epidemiological theory; a body of recent work has focused on analogies between the regional dynamics of infectious diseases and the dynamics of ecological metapopulations (Grenfell and Harwood 1997; Earn et al. 1998; Swinton et al. 1998). The twofold issues are to dissect how infection processes at the local scale determine spatiotemporal patterns of epidemics and to understand how these patterns are affected by the network of spatial spread between patches.

Spatial transmission of directly transmitted infectious diseases is ultimately tied to movement by the hosts. The network of spatial spread (the disease's spatial coupling) may therefore be expected to be related to the transportation network within the host metapopulation. In ecology, spatial coupling was classically assumed to be a simple inverse function of distance (e.g., Okubo 1980). However, metapopulation ecology has shown that both emigration and immigration rates may partially depend on patch size (Hanski 1998). For social animals in general and for humans in particular, distance-based coupling is likely too simplistic an assumption, since movement between large communities is disproportionately more common than between small ones (Erlander and Stewart 1990). Murray and Cliff (1975) and Cliff et al. (1993) proposed that such complex patterns of host movement result in what we may call "gravity transmission" (after the class of gravity models from transportation theory; Erlander and Stewart 1990).

In this study, we formulate an epidemic metapopulation model by combining the time series susceptible-infected-recovered (TSIR) model (Bjørnstad et al. 2002; Grenfell et al. 2002), which sets the standard susceptible-infected-recovered (SIR) model in a time series framework, with the gravity model for regional spread. Our goal is to estimate the parameters of the model from data and to investigate whether the model can provide a quantitative picture of how a measles metapopulation operates. We seek to understand how epidemiological coupling (the rate of spatial transfer of infection) scales with the respective sizes of "donor" and "recipient" populations, the distance between these, and what aspects of this scaling control the synchronization of epidemics to shape hierarchical infection waves (Grenfell et al. 2001). We focus on these issues on the basis of the richest data set: the urban spatiotemporal measles notification data set during the prevaccination era (weekly records for 954 locations during 1950–1966). Specifically, we develop a spatial extension of the TSIR model that assumes gravity transmission between different communities within the epidemic metapopulation. As well as giving an unusually detailed picture of the determinants of transmission at different scales, the resulting model is the most detailed metapopulation patch model to date of a specific host/natural enemy system.

Theoretical approximations to networks of spread are important for numerous reasons. First, such approximations may provide a characterization of consumer-resource dynamics in heterogeneous landscapes. Second, such networks may provide a priori models for predicting spatial spread of pathogens and may ultimately lead to improved intervention strategies (Ferguson et al. 2003; Keeling et al. 2003). Finally, recent theory suggests that the topology of contact networks is very important for the evolution of virulence (Read and Keeling 2003). Understanding the network that governs regional spread and the consequences of the resultant spatial transmission on local epidemics is the focus of our study.

A Space-Time Model

The epidemic metapopulation model represents an extension of the TSIR model (Bjørnstad et al. 2002; Grenfell et al. 2002) through the inclusion of an explicit formulation for the spatial transmission between different host communities. The nonspatial TSIR model provides a statistical link between standard theoretical models and epidemic time series data.

If we consider the epidemic dynamics through a single epidemic generation (= latent + infectious period ≈ 2 weeks for measles), the force of infection (ϕ)—that is, the rate at which a susceptible encounters infectious individuals to become infected—will be approximately constant. The probability of infection in this unit of time is $1 - e^{-\phi}$, so the expected number of new infections, λ, will be $\lambda = S(1 - e^{-\phi})$, where S is the number of susceptibles. For reasonable values of ϕ, this expectation is well approximated by $\lambda \simeq S \times \phi$, which constitutes the core of the TSIR model. (We chose to use the latter approximation because it is amenable to statistical estimation. For theoretical purposes, it may be desirable to use the former formulation [W. W. Murdoch and C. J. Briggs, unpublished manuscript].)

Demographic stochasticity introduces variability around the expected trajectory of the epidemic. Demographic stochasticity is a critical component of the dynamics because it predicts breaks in the chain of transmission, local extinction of pathogens, and community thresholds for persistence (cf. the critical community size; Bartlett 1956). Stochasticity can also exert far more subtle effects on the dynamics of infectious disease (for detailed discussion, see Rand and Wilson 1991; Rohani et al. 2002). Conditional on the numbers of susceptible and infected individuals in the previous epidemic generation, one can use two plau-

sible models for demographic stochasticity depending on the distribution of infectious periods. If the infectious period is fixed and epidemic generations separated, the chain binomial model predicts binomial variation around the expectation (e.g., Bailey 1975; Cliff et al. 1993). Alternatively, if infectious periods are exponentially distributed (as is implicitly assumed in the standard SIR models), the stochastic epidemic represents a generalized birth and death process (Kendall 1949; Bjørnstad et al. 2002). The variability is then best approximated by a piecewise constant (at the one-generation scale) birth and death process, in which case,

$$I_{t+1} \sim \text{NegBin}(\lambda_{t+1}, I_t), \tag{1}$$

where NegBin(a, b) signifies a negative binomial distribution with expectation a and clumping parameter b. This is the formulation used in the TSIR model. The negative binomial is encountered frequently in ecology. However, the above conditional distribution derives from stochastic process theory and may therefore be less familiar. The derivation is as follows (Kendall 1949): if we assume a birth and death process with a per capita growth rate, which in our case is $S \times \phi/I$, then, starting with one individual, the number of individuals one generation later will be distributed according to NegBin($S \times \phi/I$, 1). In the general epidemic setting, we start with I individuals, so the distribution one generation later will be (approximately) a sum of I negative binomials. Equation (1) follows because the sum of b NegBin(a, 1) distributions is a NegBin($a \times b$, b) (e.g., Evans et al. 1993).

The TSIR model gives a generally excellent fit to historical measles dynamics in cities and villages and sheds light on epidemical parameters and their scaling with respect to host community size (Finkenstädt and Grenfell 2000; Bjørnstad et al. 2002; Grenfell et al. 2002). In particular, the transmission rate, β, varies seasonally because of term-time forcing (Fine and Clarkson 1982) modulated by age-structured transmission (Bjørnstad et al. 2002). The average transmission rate, $\overline{\beta}$, scales inversely with community size (so-called frequency-dependent transmission) so that the force of infection ϕ scales as $\beta I/N$, where N is the community size (Bjørnstad et al. 2002).

To develop a spatially explicit version of the TSIR model, we consider the linked dynamics of K host communities (954 in the case of urban epidemics in England and Wales) of size N_k. For simplicity, we assume that N_k is constant through time. This is a rough approximation for the 1950–1965 measles case study, for which the median growth of the communities was 7.1% (78% of the 954 communities grew during the period). For consistency with previous local analyses (Bjørnstad et al. 2002; Grenfell et al. 2002), we use the population size in 1960 here. The force of infection is therefore likely to be slightly underestimated (by about 3%–4%) during the early part of the time series and slightly overestimated toward the end. Future refinements should correct for this.

In the spatially explicit model, we let $I_{k,t}$ and $S_{k,t}$ represent, respectively, the number of infected and susceptible hosts in area k at time t. The force of infection in a host community embedded in an epidemic metapopulation is a weighted average of local infection rates versus spatial contagion (Swinton 1998). For microparasites like measles (and the related phocine distemper virus; Swinton 1998; Swinton et al. 1998), frequency-dependent transmission has subtle consequences for the appropriate weighting of these two processes; the consequences of movement of susceptibles and infectious are asymmetric. This asymmetry is best illustrated by assuming that any transient (migrant susceptible or infectious hosts) is dynamically indistinguishable from local hosts during the transit. Let us consider one local community, j, and one other community, k. If spatial contagion is due to susceptible movement, the overall force of infection experienced by individuals in community j scales with $\beta[(1-\eta)I_j/N_j + \eta I_k/N_k]$, where η ($\ll 1$) is the time spent away from the home community. If, in contrast, spatial contagion is due to movement of infectious hosts, the overall force of infection scales with $\beta[(1-\eta)I_j + \eta I_k]/N_j$. In this study, we use the latter approximation. The key motivation for this is linked to its apparent success in predicting the dynamics of the epidemic measles metapopulation. Elucidating the dynamics of susceptible-driven spatial contagion or more complex movement regimes is an area of current inquiry (Keeling and Rohani 2002; Keeling et al. 2004).

Under infection-driven spatial contagion, the expected number of new cases in community k at time $t+1$ is, according to the TSIR formulation,

$$\lambda_{k,t+1} = \frac{\beta_t S_{k,t}(I_{k,t} + \iota_{k,t})^{\alpha}}{N_{k,t}}. \tag{2}$$

Here, $\iota_{k,t}$ accounts for the transient force of infection due to spatial contagion. Since migration of infected individuals is relatively rare (and unobserved), we make the approximation $(1-\eta) \approx 1$ for the local force of infection to arrive at equation (2). Note that equation (2) explicitly embraces the frequency dependence in transmission. Thus, β_t is invariant across all host communities (with estimated mean $\overline{\beta} = 29.9$, SE $= 0.99$). The transmission rate does, however, vary seasonally (see below; Bjørnstad et al. 2002). The epiphenomenological exponent, α, which usually takes a value slightly less than unity (see below), has a range of motivations. First, if individuals are spatially or socially clustered within local communities, the force of infection will be disproportionately smaller at high infec-

tious densities (Fine and Clarkson 1982; Liu et al. 1987). Second, this exponent may be seen as a correction for biases because of the temporal discretization of the underlying continuous time epidemic process (Glass et al. 2003). Finally, time series analyses support the use of such a discounting of the force of infection during epidemic peaks (Finkenstädt and Grenfell 2000; Finkenstädt et al. 2002).

The associated balance equation for the susceptibles is

$$S_{k,t+1} = S_{k,t} - I_{k,t+1} + B_{k,t}. \tag{3}$$

Here $B_{k,t}$ is the local number of new hosts born into the susceptible class. This balance was first introduced by Bartlett (1957) for measles epidemics. It is important to note that the model altogether ignores host deaths, as included in the classic epidemic model (Nåsell 1999; Hethcote 2000). This, however, is not a bad approximation; in developed countries, case fatality from measles was very low even going back to the 1950s, and before mass vaccination, almost all susceptibles were infected before the age of 20 (Anderson and May 1991). Thus, natural host mortality almost exclusively affected the recovered class.

The final consideration for local dynamics is to model the importance of transient infection. This will be a random variable with some expectation ($m_{k,t}$). Considering that transients are unlikely to stay for a full epidemic generation, we assume $\iota_{k,t}$ to take a positive but fractional (rather than integer) value:

$$\iota_{k,t} \sim \mathrm{Ga}(m_{k,t}, 1), \tag{4}$$

where $\mathrm{Ga}(m, a)$ represents a gamma distribution with shape parameter m and scale parameter a. (If transient infecteds remained for a full epidemic generation, the appropriate formulation would be $\iota_{k,t} \sim \mathrm{Poisson}(m_{k,t})$, as assumed in Bjørnstad et al. [2002] and Grenfell et al. [2002].)

Equations (1)–(4) represent the doubly stochastic TSIR model for measles epidemics. This formulation makes a number of simplifying assumptions but does capture the major interactions between epidemic nonlinearities, seasonality, and stochasticity that drive local measles dynamics (Bjørnstad et al. 2002; Grenfell et al. 2002).

Epidemic Coupling

A Gravity Model for Spatial Transmission

Spatial coupling determines the invasion speed of a pathogen across the geographic range of susceptible hosts (Bacon 1985; Mollison 1995). Furthermore, spatial coupling is the critical parameter determining phase coherence and spatial synchrony (Grenfell et al. 2001) and thereby metapopulation persistence of host-pathogen systems (Wood and Thomas 1996; Swinton 1998; Keeling et al. 2004). Both local recolonization and regional invasion are thus governed by an epidemic network that specifies the strength of coupling between different host populations. Understanding the spatial contact network for parasite transmission is thus something of a holy grail, because it will allow predictions about the spread of emerging pathogens and ultimately guide public health and veterinary intervention programs.

The quest for an appropriate spatial network translates to quantifying how $\iota_{k,t}$ depends on the size and isolation of a given host population k and the geometry of the metapopulation in which it is embedded. If transmission is through simple diffusion of infected hosts, the network may be expected to be distance (and perhaps habitat) dependent (Swinton et al. 1998; Smith et al. 2002). However, the network for human pathogens is likely to be more complex because of the intricate local and long-range movement behavior of the host (Cliff et al. 1993; Sattenspiel and Powell 1993; Grenfell et al. 2001; Lloyd and May 2001).

A standard preliminary approach would be to assume inverse or exponential distance weighting for the contact probability. However, this assumption failed to fit the measles data and does not reproduce empirical regional patterns (Y. Xia, O. N. Bjørnstad, and B. T. Grenfell, unpublished data). Instead, we build on gravity network models from transportation theory (Erlander and Stewart 1990), as proposed by Cliff et al. (1993). Detailed analyses of recreational and professional behavior by humans show that movement often depends on both the size of and distance between the communities. According to a generalized gravity model, the amount of movement between two communities k and j is proportional to $N_k^{\tau_1} N_j^{\tau_2}/d_{jk}^{\rho}$ with $\rho, \tau_1, \tau_2 > 0$, where d_{jk} is the distance between the areas. Under infection-driven spatial contagion, the transient force of infection exerted by infecteds in location j on susceptibles in location k will be

$$m_{j \to k,t} \propto \frac{N_{k,t}^{\tau_1} I_{j,t}^{\tau_2}}{d_{jk}^{\rho}}.$$

Supposing there are K host populations ($k = 1, 2, \ldots, K$) in the epidemic metapopulation, the transient force of infection will then depend on the influx from all other areas. Thus, the expectation for this quantity will be

$$m_{k,t} = \theta N_{k,t}^{\tau_1} \sum_{j \neq k} \frac{I_{j,t}^{\tau_2}}{d_{k,j}^{\rho}}, \tag{5}$$

where θ measures the spatial coupling strength. The pa-

rameter τ_1 determines how attraction to an area scales with size ($\tau_1 = 1$ means that attraction is proportional to recipient community size; $\tau_1 < 1$ means that attraction scales slower than proportional with size, etc.). The parameter τ_2 quantifies how the transient "emigration" intensity scales with donor population size. Finally, ρ quantifies how attraction decays with distance.

Theoretical Dynamics

Equations (1)–(4) with a spatial network according to equation (5) represent a fully specified space-time model for an epidemic metapopulation. However, its behavior depends critically on a set of gravity parameters that influence the spread of infection in complex ways. Before applying the model to the prevaccination dynamics of measles, we therefore investigate how the spatial dynamics of a "measles-like" pathogen depends on the coupling parameters in equation (5) using a simplified spatial map of host populations. We consider a large central core city ($N_0 = 5{,}000{,}000$) surrounded by 500 smaller "satellites" with host population size 100,000 (fig. 1*a*). We take the per capita birthrate to be 0.017 year^{-1} for all the cities (Finkenstädt et al. 1998; Bjørnstad et al. 2002). We further assume measles-like parameters for the local transmission dynamics (eqq. [1]–[3]): $\alpha = 0.97$, $\beta_t = 24.6$ for non-school time (i.e., first, eighth, fifteenth, sixteenth, seventeenth, eighteenth, nineteenth, twenty-third, twenty-sixth biweeks), and 33.3 for term time.

We subsequently vary the gravity model parameters through a sequence of simulations of the doubly stochastic metapopulation model (each of 2,000 iterations). In each case, we explored two key quantities (Grenfell et al. 2001)—the relative phase angle of the epidemics and the epidemic synchrony—as functions of the distance from the core city. We estimate the former using wavelet phase analysis (Grenfell et al. 2001) and the latter as the correlation between time series. In the following theoretical exploration, we reduce the dimension of system complexity by assuming that $\tau_1 = 1$ (Cliff et al. 1993). (In later statistical analysis of the measles data, we will relax this assumption to estimate all four gravity parameters.) In this way, we investigate the dynamical impact of overall coupling strength (θ), the decay exponent of coupling with

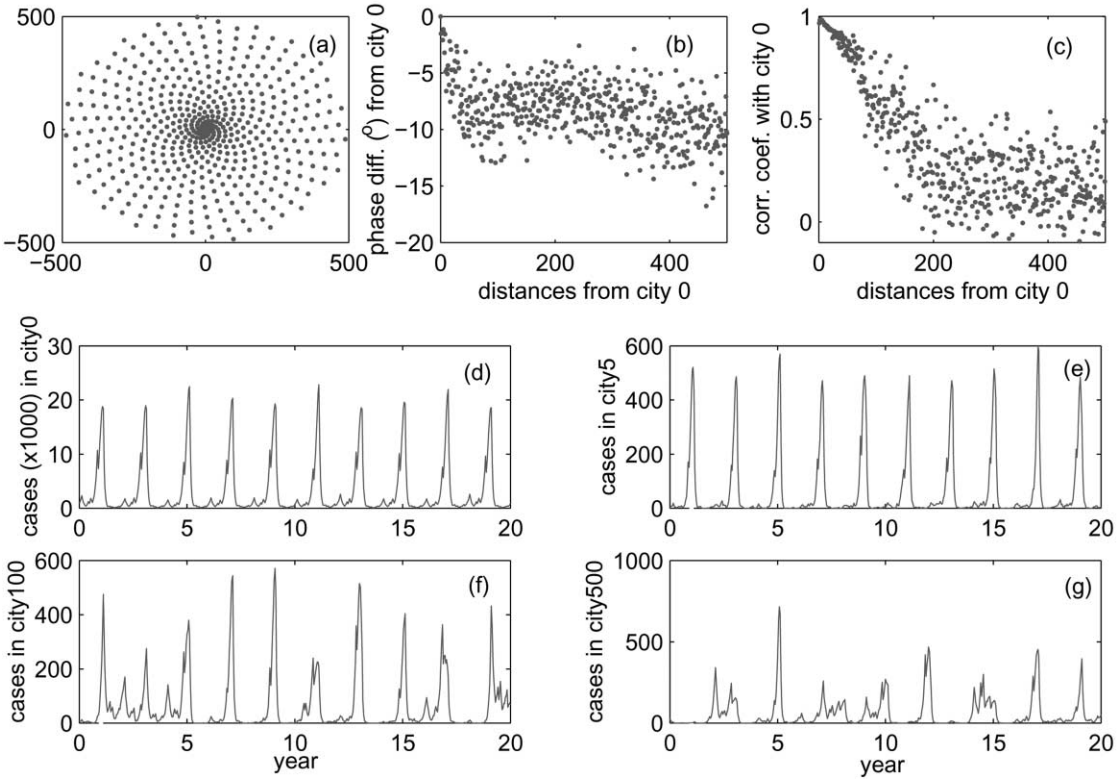

Figure 1: Epidemics on an artificial landscape. *a* is the geographic position of the 501 cities. *b* and *c* are the phase difference and the correlation coefficients, respectively, of the 500 satellites with the core city (180° phase difference corresponds to major biennial epidemics completely out of phase). *d*–*g* are typical realizations of the model in different cities.

distance (ρ), and the "donor" population exponent (τ_2). As a first illustration, figure 1*d*–1*g* shows epidemic dynamics in the core city (0) and cities 5, 100, and 500, assuming that $\theta = 0.01N_0^{-1}$, $\rho = 1$, and $\tau_2 = 1$. The dynamics of the core city are virtually unaffected by immigrants, since there are many local infectious individuals (even in the epidemic troughs); the epidemic trajectory for highly contagious pathogens is insensitive to transient infection as soon as the local number of infecteds is more than a handful (Bjørnstad et al. 2002). Satellite communities close to the core exhibit epidemics that are highly correlated with the core dynamics (fig. 1). However, as distance from the core increases, the degree of synchrony declines and the phase difference expands, testifying to the presence of spatial waves away from the core city (Grenfell et al. 2001). Peripheral communities exhibit irregular epidemics with long periods of pathogen extinction.

In figure 2, we consider the effect of epidemic coupling on phase relations and synchrony through varying the parameters in the gravity model. As coupling (θ) increases (fig. 2*a*, 2*b*), the influence of the core city on local dynamics is magnified. Whenever the flux of transient infection from the core is sufficiently large (such as in central cities, e.g., city 1), the dynamic pattern of the satellite city mirrors that of the core. In the metapopulation as a whole, increased coupling tends to reduce the phase difference between cities (fig. 2*a*) and increase the overall synchrony (fig. 2*b*). As ρ increases, in contrast, the decay in coupling with distance rises. The phase difference therefore drops more rapidly with distance, and the geographic extent of the hierarchical waves (as judged from the decay in synchrony) appears to decrease (fig. 2*c*, 2*d*). As τ_2 increases, the core city donates disproportionately more infections to the satellite cities and thus magnifies the overall coupling. As a consequence, the phase difference becomes

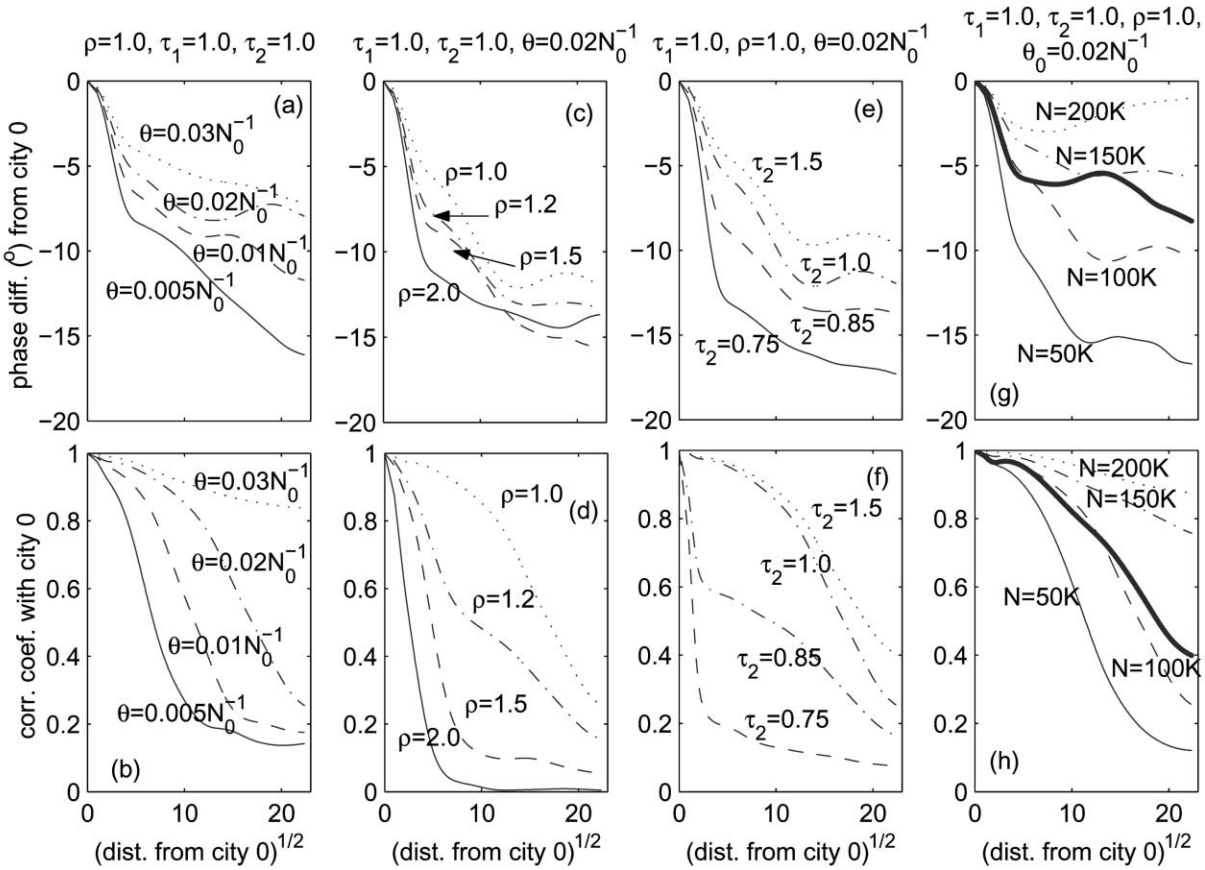

Figure 2: Spatiotemporal dynamics and parameter variation in an artificial epidemic landscape. *a–f* are nonparametric smoothers of the correlation coefficients between time series in city 0 and the other cities and phase difference between city 0 and the other cities. In *g* and *h*, different lines correspond to population sizes for all the "satellites" 50,000, 100,000, 150,000, and 200,000, respectively. For the solid lines, the population decreases from 200,000 for the city closest to city 0 to 50,000 for the farthest city.

more shallow, and overall synchrony is enhanced (fig. 2*e*, 2*f*).

A final important modulator of the spatial dynamics is the average size of the host communities and the degree of heterogeneity in size. Comparing the thin lines in figure 2*g* and 2*h*, we find that the phase difference increases as peripheral populations decrease in size. By contrast, as peripheral communities approach the critical community size, the epidemics become increasingly phase locked (see also Grenfell et al. 2001).

The most important empirical deviation from the basic core satellite arrangement used in most of figure 2 is that there tends to be spatial clustering around large cities; the size of the communities tends to decrease with distance from core cities (Grenfell et al. 2001). We therefore also studied the consequences of having a gradient in community size away from the core (*bold lines*, fig. 2*g*, 2*h*). Both phase differences and decay in spatial synchrony show intermediate patterns to the constant-sized satellites. However, the synchrony and phase differences indicate that the smallest most peripheral communities are less epidemiologically isolated in the hierarchical case. This is because of their gravity coupling to relatively close and relatively large intermediate communities.

In summary, the proposed spatiotemporal model (eqq. [1]–[5]) holds the potential to capture diverse aspects of epidemic metapopulation dynamics (for caveats, see "Discussion") depending on model parameters. These features include local oscillatory dynamics, local extinction in small communities, phase differences in the timing of epidemics, and the degree of synchrony of epidemics. Armed with these insights, we now turn to a more detailed consideration of the metapopulation dynamics of measles on a real host geography. The issues are twofold: first, can we estimate the parameters from the data? Second, given parameter estimates, does the TSIR/gravity formulation capture the essence of the space-time dynamics of measles?

Measles Metapopulation Dynamics in England and Wales

Data

Weekly case reports of measles for the 954 urban locations in England and Wales from 1944 to 1967 represent a particularly useful case study of spatiotemporal epidemic dynamics (Grenfell et al. 2001). There is a well-understood underreporting bias of 40%–55% in these records (Bjørnstad et al. 2002). Allowing for this, however, the records are complete, and they reveal spectacular interannual (usually biennial) outbreaks of infection. A critical feature of this epidemic metapopulation is that, except for a handful of large Type I cities (>300,000 inhabitants), infection frequently goes locally extinct, so that overall persistence hinges on episodic reintroduction and spatial coupling. Before further analyses, we corrected the reported data by a factor of 1/0.52, with 52% being the average reporting rate in previous analyses.

For simplicity, we assume that the population sizes and per capita birthrates are approximately constant throughout the time considered and take them as those in 1960 for each of the 954 areas. This is a crude approximation, since most communities grew during the period (reviewed above). The force of infection is, therefore, on average slightly underestimated (overestimated) during the early (late) part of the study.

Fitting the Gravity TSIR Model

The parameters governing local transmission of measles (eqq. [1]–[3]) were previously estimated from a subset represented 60 communities (spanning almost three orders of magnitude in size; Bjørnstad et al. 2002; Grenfell et al. 2002). The estimates have since been validated for all 954 communities (O. N. Bjørnstad and B. T. Grenfell, unpublished data). We will use these estimates for the spatial analysis. In particular, the seasonal transmission rates for biweeks 1 through 26 are $\beta_t = 30$ (1.24, 1.14, 1.16, 1.31, 1.24, 1.12, 1.06, 1.02, 0.94, 0.98, 1.06, 1.08, 0.96, 0.92, 0.92, 0.86, 0.76, 0.63, 0.62, 0.83, 1.13, 1.20, 1.11, 1.02, 1.04, 1.08), and α will be taken to be 0.97. The current challenge is to quantify the parameters of the gravity model (eq. [5]) and thereby provide a quantitative description of the topology of the epidemic network.

Simultaneous estimation of all four gravity parameters is difficult, first, because of the inherent collinearity, especially between parameters τ_1, τ_2, and ρ. We simplify this problem through sequential estimation of the parameters. We will initially assume that the parameters τ_1 and ρ are unity, and we estimate θ and τ_2 conditional on this assumption; we then estimate the former on the basis of the latter fits. More broadly, however, the estimation of the parameters is a formidable statistical problem because we are trying to match complex spatiotemporal dynamics in a heterogeneous landscape. This means that there are several potential "objective functions"—measures of the statistical distance between the data and the model—that may be minimized to estimate the parameters. The classic solution is to optimize short-term forecasting and minimize one-step-ahead prediction error (Tong 1990). However, from an ecological point of view, long-term spatiotemporal signatures may be equally or more important (for a general ecological discussion, see Kendall et al. 1999). In particular, an appropriate model for the epidemic metapopulation model should get epidemic sizes (Finkenstädt et al. 2002), fade-out lengths (Grenfell et al. 2002), relative phase re-

lationships, and patterns of spatial synchrony right (Grenfell et al. 2001).

We approach the problem here with a somewhat ad hoc approach; we combine minimizing short-term prediction error with matching key long-term signatures. We have found that this provides a reasonable characterization of feasible parameter values. However, it also raises a number of future methodological questions. We return to these in "Discussion."

Short-Term Prediction. Minimizing one-step-ahead prediction error is the method most commonly used to estimate epidemiological parameters for the TSIR and other nonlinear time series models for ecological dynamics (Ellner et al. 1998; Bjørnstad et al. 2002). The methodology is based on comparing one-step predictions of the models with observed equivalents. Here, we use the classic loss function, the simple (conditional) least squares formulation:

$$L(\theta, \tau_1, \tau_2, \rho) = \sum_k \frac{1}{N_k} \sum_{I_{k,t}>0} \frac{[y_{k,t} - \hat{y}_{k,t}(\beta_t, \theta, \tau_1, \tau_2, \rho)]^2}{T_k}.$$

Here $y_{k,t} = \log(I_{k,t})$, β_t is the previously estimated seasonally transmission rate, $\hat{y}_{k,t}()$ is the one-step-ahead prediction of $y_{k,t}$ based on equations (1)–(5) and candidate gravity parameters, and T_k is the number of nonzero observations for I_k in the time series. The final $1/N_k$ weighting has deeper motivations; previous analyses of the TSIR model showed that the influence of infectious influx on the overall epidemic trajectory is proportional to $\beta_t \iota_t / I_t$ (Bjørnstad et al. 2002). On average, I_t is proportional to N; thus, in order to quantify spatial contagion, it is appropriate to use a $1/N$ weighting scheme.

Figure 3*a*–3*c* shows the value of the least squares loss function for various parameter combinations of θ, τ_1, τ_2, and ρ. This calculation puts τ_1 near unity, τ_2 around 1.5, and ρ close to 1. Over and above this, the analysis reveals how the one-step-ahead analysis provides little information with respect to the epidemic coupling parameter, θ. This parameter appears to be elusive from the point of view of the one-step-ahead method.

Estimation Based on Long-Term Dynamics. There are several potential distance measures between the model and the long-term spatiotemporal patterns in the data, which all could be used as alternative tools to estimate spatial parameters (notably θ). Because of the sensitive dependence of epidemic correlation on the gravity parameters (fig. 2), we estimate θ by minimizing the predicted and observed epidemic synchrony within the spatiotemporal data panel (Fuller 1976; Whitcher et al. 2000). (Optimizing wavelet phase angles would represent a viable alternative [fig. 2]. However, the computational overhead is substantial for wavelet decomposition; we therefore focus on spatial correlation in this study.) To simplify calculations, we use the predicted correlation between the epidemics of the 954 communities and the epidemic trajectory observed for London. Let r_k be the correlation coefficient between nonzero case reports in area k and London, and let $\hat{r}_k(\theta, \tau_1, \tau_2, \rho)$ be the predicted correlation based on the model. An appropriate loss function based on deviations in observed and predicted correlations is

$$R(\theta, \tau_1, \tau_2, \rho) = \sum_{k=1}^{954} \frac{|r_k - \hat{r}_k(\theta, \tau_1, \tau_2, \rho)|}{954}.$$

Given $\rho = 1$, $\tau_1 = 1$, and $\tau_2 = 1.5$, this loss function reveals a well-behaved estimate for θ near $0.015 N_{\mathrm{LD}}^{-1}$ (fig. 3*d*), where N_{LD} is the population size of London.

Validation and Prediction

The acid test for the gravity model is to compare its predictions of long-term dynamics with those observed in measles. We have already used aspects of the spatiotemporal correlation structure of measles to estimate the overall coupling strength, θ. We now test the model against other key temporal and spatial features of measles dynamics: how measles incidence scales with population size, the periodicity of recurrent epidemics, patterns of extinction and recolonization in the epidemic metapopulation, and hierarchical waves and phase relations around large centers. We compare the model predictions with data for each of these in turn.

We first compare the overall numerical scale of epidemics in all the towns and cities of England and Wales (fig. 4*a*–4*c*). The numbers of observed and predicted cases scale very similarly with populations size. Next, we compare the cyclic patterns among towns. Prevaccination measles dynamics display a mixture of biennial (cyclic) and annual (seasonal) dynamics in large cities, with more irregular 2–3-year cycles in small towns (Bartlett 1956; Bjørnstad et al. 2002; Grenfell et al. 2002). We crudely quantify the balance of the seasonal and interannual—generally biennial—variation on the basis of spectral analysis of observed and simulated epidemic time series. Spectral analysis is fraught with estimation uncertainty; for example, the periodogram does not provide a consistent estimate of the spectral density (Priestley 1981). We therefore measure relative importance of the seasonal versus interannual cycles as the ratio of the summed power of fluctuations with 0.5–1.5-year periods ("seasonal variation") to the summed power of those with 1.5–2.5-year periods (biennial vari-

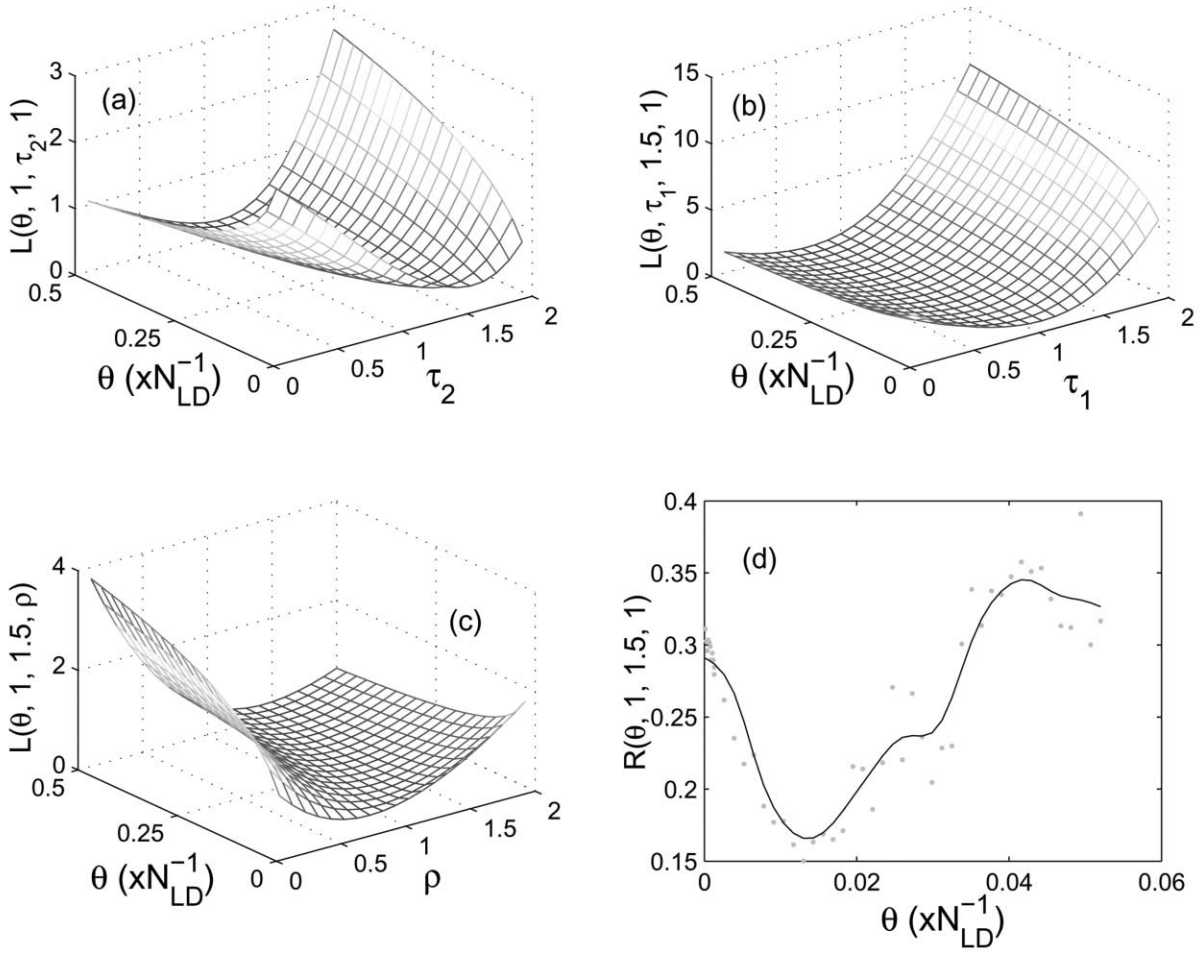

Figure 3: Estimation of gravity TSIR model from short-term dynamics. In *a*, the loss function $L(\theta, 1, \tau_2, 1)$ achieves its minimum point around $\tau_2 = 1.5$. In *b*, $L(\theta, \tau_1, 1.5, 1)$ achieves its minimum point around $\tau_1 = 1$. In *c*, $L(\theta, 1, 1.5, \rho)$ achieves its minimum point around $\rho = 1$. *d* shows the very shallow loss function $R(\theta, 1, 1.5, 1)$ at different values of θ by points. The curve is a nonparametric kernel smoother of the points. The loss function $R(\theta, 1, 1.5, 1)$ achieves its minimum point around $0.015N_{\mathrm{LD}}^{-1}$, where N_{LD} is the population size of London. (Color version of figure available in the online edition of the *American Naturalist*.)

ation; Bolker and Grenfell 1995; fig. 4*d*–4*f*). The model, again, appears to reflect the observed scaling of local dynamics; both observed and simulated series show an overall progression to dominantly biennial cycles with increasing community size.

Third, we compare the observed and predicted scaling of epidemic extinction rates ("fade-outs"; fig. 4*g*–4*i*). We measure the overall extinction rate by the proportion of zeros in the time series: more sophisticated measures (Bartlett 1960) give similar results (not shown). Again, the qualitative fit is good: both the model and the data reflect the well-known increase in persistence with population size. In more detail, the scatterplot of observed and simulated fade-outs shows a slight bias; over much of the range of population sizes, the simulated series show slightly more fade-outs than observed. This may partly be due to the greater stochastic variation (and therefore greater decorrelation of epidemic troughs) in the real system. It may conceivably also be influenced by subtleties relating to the underreporting in the data. Intuitively, this would lead to the reverse bias, though.

In the appendix in the online edition of the *American Naturalist*, we provide further comparisons between predicted and observed dynamics. On the whole, the phase relationships predicted by the epidemic metapopulation model compare very well with those observed in the data. The phase relations do, however, depend critically on the gravity exponent, ρ. Small values of ρ lead to phase locking

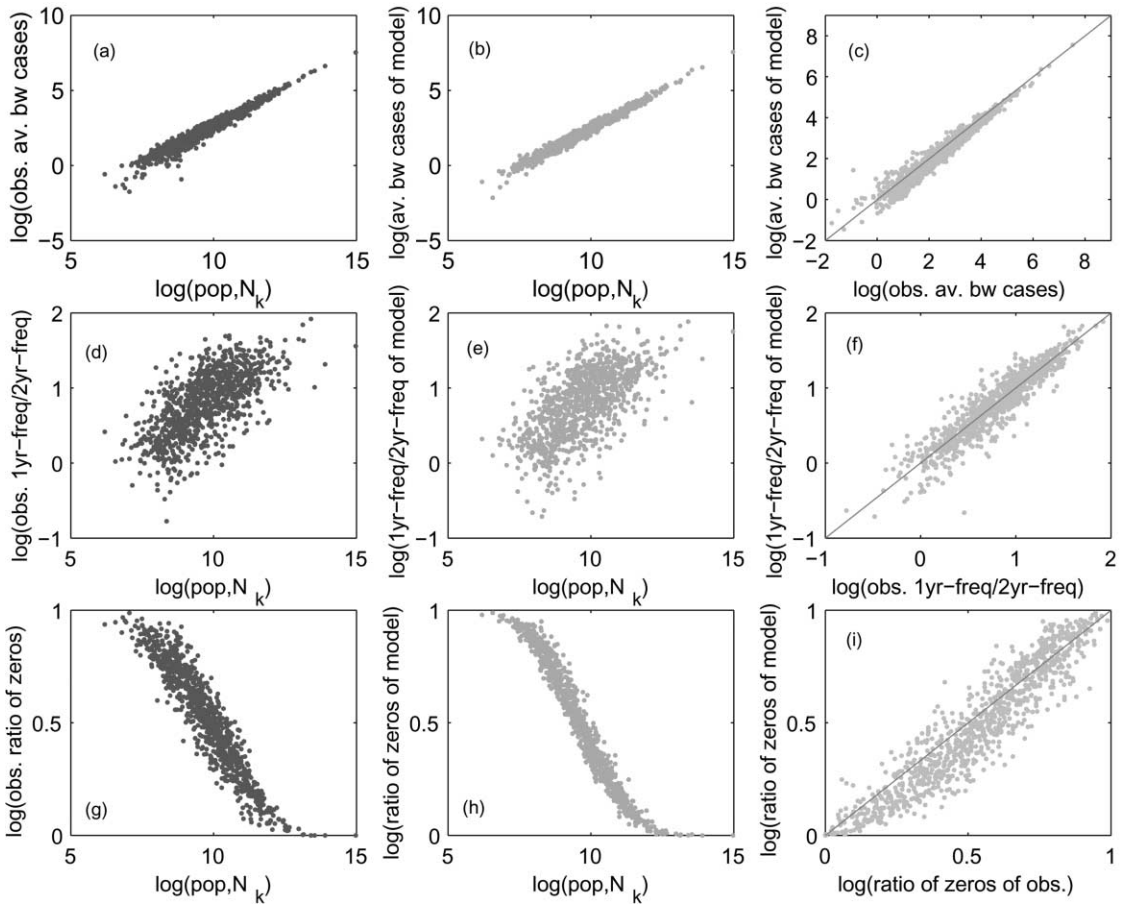

Figure 4: Comparison of observed and predicted prevaccination measles incidence and persistence in England and Wales as a function of urban population size. The observations were taken from 1944 to 1967 in 954 urban areas. *a–c* are the average number of biweekly cases in the 954 urban areas. *d–f* are the ratios of biennial to annual cycle frequencies. *g–i* are the proportion of zeros in the time series. For each row, the first and second panels are based on the observations and model, respectively; the third panel shows equivalent scatterplots of observed and model results; the straight line is $y = x$. (Color version of figure available in the online edition of the *American Naturalist*.)

of all epidemics (i.e., zero phase differences). This is because the system approaches the mean field as ρ approaches 0. Our estimate of ρ near unity gives regional dynamics comparable to those seen in the data. Higher values of ρ near the "diffusion" limit of 2 (Murray and Cliff 1975; Cliff et al. 1993) also produce reasonably good qualitative fits to the phase dynamics. However, as discussed in the theoretical exploration (fig. 2), such values of ρ lead to rapid decays in correlation with distance.

Mapping Epidemiological Isolation

The gravity formulation represents a simple model for the regional epidemic network. When combined with the TSIR model, this formulation appears to successfully predict the spatiotemporal dynamics of measles. It is interesting to ask what the emergent network topology predicts about epidemiological isolation (and, conversely, epidemiological coupling) in the real (and heterogeneous) epidemic metapopulation. There are two key quantities to consider. First, the recipient perspective: what is the influx of infection into any given community? Second, the donor perspective: how much transient infection does a given community export to the metapopulation at large?

The intermediate values of the gravity exponents ρ, τ_1, and τ_2 result in hierarchical localization of dynamics around the core areas represented by the communities above the critical community size. This is best illustrated by mapping the per capita infectious "import" and "export" rates of the different communities (fig. 5). On the whole, the aggregations of communities that, on a per capita basis, most fuel the epidemic metapopulation (fig. 5*b*) are also the ones that see the greatest infection influx (fig. 5*a*). This is partly because of the approximate bilin-

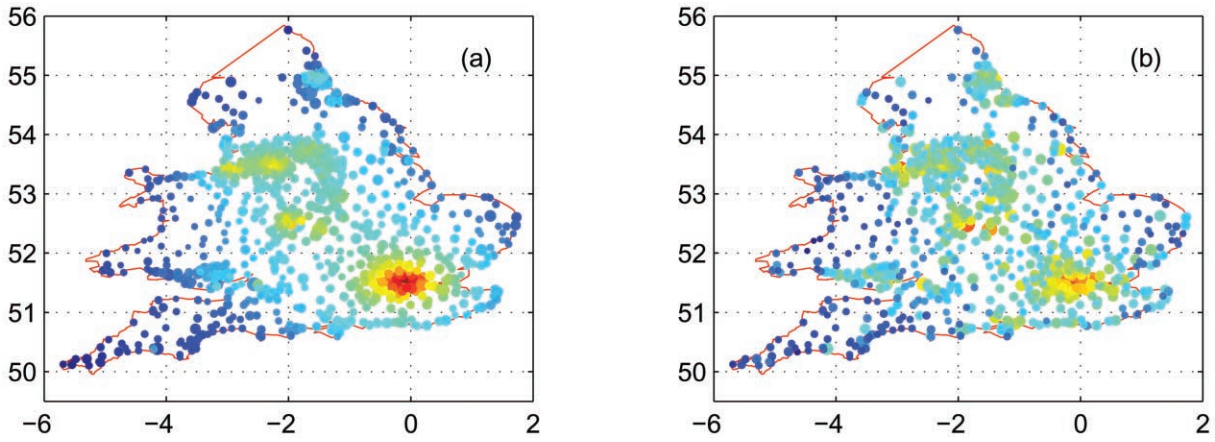

Figure 5: Epidemical isolation in the model measles population. *a*, Per capita influx of infections from all the other areas. *b*, Per capita emigrants from the area. The values of the per capita influx or emigrants (from low to high) are indicated by color from blue to cyan to yellow to red.

earity inherent in gravity networks. However, equally important is the spatial autocorrelation in community size; communities in the vicinity of the core areas tend to be larger than the more peripheral towns. Thus, the large urban centra (London, Birmingham, and the industrial northwest) and the communities around them fuel the epidemic traveling waves through both receiving and donating more transient infection than the more peripheral satellite communities. This is as compared with, say, the relatively small and isolated communities in parts of Cornwall and mid- and North Wales (fig. 5; see also Grenfell et al. 2001).

Discussion

The theory of metapopulation dynamics has been acclaimed for elucidating many of the key issues of landscape and conservation ecology (e.g., Hanski 1998). It is increasingly recognized that analogous extinction/recolonization processes may underlie dynamics of a range of often intrinsically unstable consumer-resource systems. Parasitoids (e.g., Murdoch 1994) and pathogens (e.g., Grenfell and Harwood 1997) are particularly striking examples. For theoretical ecology, this realization is both a blessing and a curse: it promises deeper understanding of interactions that are inherently spatiotemporal, and at the same time, it crystallizes a new challenge: the need to characterize the rate of spatial contact between different host communities. Predicting spread and persistence of acute viral infections will ultimately require an understanding of the topology of the underlying network of spatial contagion. The fact that the details of the spatial networks are important is emphasized by two different lines of enquiry. First, many strategies for optimal intervention have been shown to depend critically on pattern of spread (Keeling et al. 2003). Second, the question of whether evolution will favor more or less virulent strains may depend on the detailed pattern of spatial contagion (Read and Keeling 2003).

The coupling of spatially extended ecological systems has been a recent and active area of research in population ecology (Tilman and Kareiva 1997; Hanski 1998; Dieckmann et al. 2000). Using spatial diffusion as a first principle (e.g., Okubo 1980), dispersal distances will be inversely dependent on distance. Typically, dispersal distance distributions will follow exponential/Bessel (depending on whether dispersal is one-dimensional or two-dimensional) or Gaussian models (Bjørnstad and Bolker 2000). Generalizing from detailed distributional assumptions, theory predicts spatial coupling to be inversely distant dependent (e.g., Okubo 1980). Measles qualifies this: spatial coupling appears not to follow a simple distance-dependent network in mobile social "animals" (namely humans) inhabiting heterogeneous landscapes.

A central question in host/natural enemy dynamics and, indeed, in ecology in general is how to characterize the scaling of interactions in space and time (Dieckmann et al. 2000). Here we show that a gravity model, originally derived in spatial geography and sociology (Erlander and Stewart 1990), gives an accurate description of the spatiotemporal flux of measles infection in the prevaccination England and Wales data set. Measles in England and Wales provide a unique opportunity to test the "gravity" spread of a pathogen across patchily distributed host communities. In a prescient article, Murray and Cliff (1975) proposed a gravity model for measles spread around Bristol (see also Cliff et al. 1993; Thomas 1999). Here, we have extended the comparison to the full prevaccination England and Wales data set. The TSIR formulation also allows

us to quantify the balance of forces between local seasonality, nonlinear epidemic dynamics, and regional coupling. Because estimation requires nonstandard analyses, this study is admittedly preliminary (see below). However, we have been able to establish feasible ranges for the gravity parameters from the point of view of balancing long- and short-term dynamics.

Epidemic coupling appears to scale inversely with distance rather than the inverse squared distance scaling that is predicted by random diffusion (Caffrey and Isaacs 1971). A value of $\rho = 1$ corresponds to what one would expect if transportation of measles is not a spatially random diffusion process (in which case, ρ would be equal to 2) but rather due to the directed movement along the fastest—oftentimes almost straight—route to a target location (e.g., friends, family, or day care/school) but with the caveat that near targets are preferred over distant ones. This is a reasonable conclusion if we remember that measles, particularly in the prevaccination era, was restricted almost completely to children in primary school and preschool children. Here, diffusive movement (with a scaling of $\rho = 2$) may be a less adequate model than more direct movement patterns. Examination of this hypothesis using explicit movement data will be a fruitful direction for future work.

The exponent τ_2 controls the scaling of transfer of infection as a function of donor population density. Our estimation based on short-term fitting and long-term dynamic comparisons suggests that $\tau_2 = 1.5$ (>1); this implies that large centers are disproportionately important in "donating" infection to the hinterland (because coupling increases faster than linear with community size). This may happen if larger centers are disproportionately attractive in terms of social and recreational facilities, though exploring this will require models that encompass the complexities of susceptible as well as infected movement. Simulations of epidemics on artificial landscapes (not shown) illustrate how any clustering in community size can reenforce the strength and spatial extent of hierarchical waves. Exploring these issues and, in particular, their implications for disease control and the spread of emergent infections will be an important avenue for further inquiry (Ferguson et al. 2003).

In order to narrow the gap between theoretical differential equations for the mechanism of epidemics and discrete-time observations, we developed discrete-time models. Generic methodologies to estimate these time series models have not been fully investigated (Ellner et al. 1998; Finkenstädt and Grenfell 2000; Finkenstädt et al. 2002). The estimation difficulty includes the following aspects: some of the variables, such as the number of susceptible hosts in our model, are not directly observed; unrealistic assumptions, such as stationarity, are at least partially implicit in the methods; finally, there is great collinearity among some of the parameters. Most statistical methods for fitting dynamical models to data are based on minimization of a loss function related to the one-step-ahead prediction error. This minimization is, however, not synonymous with optimizing the match of the model to long-term behavior of the system (e.g., Ellner and Seifu 2002). In this article, we used both one-step-ahead prediction and long-term behavior to obtain estimates of the parameters. Using simulations, the reconstruction of the unobserved variable (susceptibles) and the estimation of the parameters may be done simultaneously. Similar ideas have been explored in applied statistics (Hannan 1973). This approach can be extended to more general cases with nonstationary dynamics; we shall discuss such estimation in subsequent articles.

The difficulty in estimating spatial coupling is partly rooted in the fact that transient infection does not necessarily have significant dynamical consequences. For example, our recent calculations (Bjørnstad et al. 2002, their fig. 9*b*) show that epidemic immigration sometimes has negligible dynamical consequences; for measles, such transient infection is dynamically unimportant as soon as local prevalence passes five to 10 infected hosts. This threshold is only crossed in small centers during the troughs between epidemics: during the prevaccination era, large cities that were above the critical community size almost always have case counts above this minimum. Thus, the trough behaviors in places below the critical community size give reliable information on coupling (Finkenstädt et al. 1998). To improve the statistical estimation, we are currently exploring whether fade-out lengths and extinction-recolonization rate carry more direct signatures of coupling rates and coupling parameters.

For simplicity, we fixed the local population exponent of the gravity model to unity; $\tau_1 = 1$ corresponds to the original findings of Bartlett on the scaling of immigration of infection against local population size (Bartlett 1957). This is the appropriate assumption if the probability of susceptibles acquiring nonlocal infection, either locally (from transient infectious individuals) or through infection while traveling, depends on density of infected individuals. Its adequacy hinges on whether the transients, either infectious or susceptible individuals, play similar roles to the resident (infectious or susceptible) individuals. In the face of differing host community sizes, this will hold only if two additional assumptions are fulfilled. First, the basic reproduction ratio, R_0, needs to be invariant of community size. We have previously showed that this is the case for measles in England and Wales (Bjørnstad et al. 2002, their fig. 8). Second, transmission has to be density dependent. If transmission is not density dependent (but frequency dependent, as is the case for measles), equation

(2) will hold only if spatial contagion is primarily driven by the transient movement of infectious individuals. (This is discussed in detail in "A Space-Time Model.") Our formulation employs one further simplifying assumption that is worth stressing: the local force of infection is not adequately discounted by any transient movement (Swinton 1998; Swinton et al. 1998). The ultimate mechanistic model needs not only to correct the force of infection for transient immigration, as done in our current formulation, but also to make the balancing corrections for transient emigration. However, as pointed out by Keeling and Rohani (2002), to do this for complex networks is nontrivial and a challenge for the future. In the current setting, spatial transmission is likely to be relatively rare. This, in addition to the apparent predictive success of our model, makes us confident that our formulation is not a bad approximation, for now.

Understanding the size and duration of epidemics is a key issue for locally nonpersistent pathogens such as measles (Nåsell 1999). High rates of transient infection may very well extend the duration of an epidemic. However, for measles, there are several reasons why this is not likely to be of great importance in the regionally endemic settings. First, spatial transmission appears to be rare. Second, the influence on local dynamics of transient infection is unimportant as soon as there are more than a handful of local infecteds (above). Finally, because of measles' high R_0, extinction is through the more or less deterministic exhaustion of susceptibles (Grenfell et al. 2002). Slight stochastic increases in the force of infection toward the end of an epidemic will have a negligible effect on the epidemic trajectory. In contrast, rates of transportation have important consequences for the overall metapopulation persistence and the time to extinction for the regional epidemic (Keeling et al. 2004). When spatial coupling is low, epidemic recolonization will be rare, making regional ("metapopulation") extinctions more common. When the coupling is high, in contrast, rates of local epidemic extinct will be somewhat diminished. However, because of the synchronizing effect of spatial transmission, epidemic declines will become aligned and therefore increasingly prone to simultaneous extinctions. Hence, regional persistence is greatest at intermediate coupling (Keeling et al. 2004).

Although the gravity model captures many of the overall features of epidemic dynamics in space and time, there are a number of important regional patterns that we still fail to match. In particular, we cannot yet represent either the tendency for epidemics in northwestern English conurbations to lead those in other centers or the dramatically anomalous behavior of Norwich and its environs in north Norfolk, where epidemics were completely out of phase with the major tendency in the rest of the country during the 1940s and 1950s (Grenfell et al. 2001). Preliminary work indicates that we may be able to address these issues using models that take explicit account of epidemics in the less dense rural areas that lie between urban centers. Sparsely populated regions appear to act as barriers to local diffusion of measles and may act to channel and isolate the epidemics in urban centers. Explicit consideration of the epidemiological impact of regional transport connections and topography is also an interesting area for future study; a major challenge for future work is to extend the model to the more complex dynamics observed in the vaccine era where, paradoxically, data for England and Wales were much more coarsely spatially sampled.

In conclusion, much of the complex prevaccination spatiotemporal behavior of the measles oscillator can be explained by conceptually simple stochastic models, which capture the balance between local dynamics and regional coupling arising from human contact networks. Because of the unique characteristics of measles, this is the most detailed such model to date. Perhaps ironically, historical patterns of human movement are far from perfectly documented. Thus, analyses of diseases records may also give unusual perspectives on the underlying flux of human movement. Furthermore, it remains to be seen whether gravity models may be of wider application in other ecological systems. Intriguingly, Schneider et al. (1998) recently showed that the spread of invasive mussels is sufficiently tightly linked to human vectoring and that the risk of spread is given by the gravity network created by boat use. We believe gravity models may ultimately provide insights into metapopulation dynamics of "nonhuman" animals with complex social organization.

Acknowledgments

L. Warlow and two anonymous reviewers provided valuable comments on the article. This work was supported by the Wellcome Trust (Y.X. and B.T.G.), the Biotechnology and Biological Sciences Research Council (B.T.G.), and National University of Singapore Faculty Research Committee R155000032112 (Y.X.).

Literature Cited

Anderson, R. M., and R. M. May. 1991. Infectious diseases of humans: dynamics and control. Oxford University Press, Oxford.

Bacon, P. J. 1985. Population dynamics of rabies in wildlife. Academic Press, London.

Bailey, N. T. J. 1975. The mathematical theory of infectious diseases and its application. Griffin, London.

Bartlett, M. S. 1956. Deterministic and stochastic models for recurrent epidemics. Pages 81–109 *in* Proceedings of the Third Berkeley Symposium on Mathematical Sta-

tistics and Probability. University of California Press, Berkeley.

———. 1957. Measles periodicity and community size. Journal of the Royal Statistical Society A 120:48–70.

———. 1960. The critical community size for measles in the United States. Journal of the Royal Statistical Society A 123:37–44.

Bjørnstad, O., and B. Bolker. 2000. Canonical functions for dispersal-induced synchrony. Proceedings of the Royal Society of London B 267:1787–1794.

Bjørnstad, O. N., B. Finkenstädt, and B. T. Grenfell. 2002. Dynamics of measles epidemics: estimating scaling of transmission rates using a time series SIR model. Ecological Monographs 72:169–184.

Bolker, B. M., and B. T. Grenfell. 1995. Space, persistence and the dynamics of measles epidemics. Philosophical Transactions of the Royal Society of London B 348:309–320.

Caffrey, J., and H. H. Isaacs. 1971. Estimating the impact of college or university on the local economy. American Council on Education, Washington, D.C.

Cliff, A. D., P. Haggett, and M. Smallman-Raynor. 1993. Measles: an historical geography of a major human viral disease from global expansion to local retreat, 1840–1990. Blackwell, Oxford.

Dieckmann, U., W. H. Lawton, and J. A. J. Metz. 2000. The geometry of ecological interactions: simplifying spatial complexity. Cambridge University Press, Cambridge.

Dietz, K. 1976. The incidence of infectious diseases under the influence of seasonal fluctuations. Lecture Notes in Biomathematics 11:1–15.

Earn, D. J. D., P. Rohani, and B. T. Grenfell. 1998. Persistence, chaos and synchrony in ecology and epidemiology. Proceedings of the Royal Society of London B 265:7–10.

Earn, D. J. D., P. Rohani, B. M. Bolker, and B. T. Grenfell. 2000. A simple model for complex dynamical transitions in epidemics. Science 287:667–670.

Ellner, S. P., and Y. Seifu. 2002. Using spatial statistics to select model complexity. Journal of Computational and Graphical Statistics 11:348–369.

Ellner, S. P., B. A. Bailey, G. V. Bobashev, A. R. Gallant, B. T. Grenfell, and D. W. Nychka. 1998. Noise and nonlinearity in measles epidemics: combining mechanistic and statistical approaches to population modeling. American Naturalist 151:425–440.

Erlander, S., and N. F. Stewart. 1990. The gravity model in transportation analysis: theory and extensions. International Science, Netherlands.

Evans, M., N. Hastings, and B. Peacock. 1993. Statistical distributions. Wiley, New York.

Ferguson, N. M., M. J. Keeling, W. J. Edmunds, R. Gant, B. T. Grenfell, R. M. Amderson, and S. Leach. 2003. Planning for smallpox outbreaks. Nature 425:681–685.

Fine, P. E. M., and J. A. Clarkson. 1982. Measles in England and Wales. I. An analysis of factors underlying seasonal patterns. International Journal of Epidemiology 11:5–15.

Finkenstädt, B. F., and B. T. Grenfell. 2000. Time series modeling of childhood diseases: a dynamical systems approach. Journal of the Royal Statistical Society C, Applied Statistics 49:187–205.

Finkenstädt, B. F., M. J. Keeling, and B. T. Grenfell. 1998. Patterns of density dependence in measles dynamics. Proceedings of the Royal Society of London B 265:753–762.

Finkenstädt, B. F., O. N. Bjørnstad, and B. T. Grenfell. 2002. A stochastic model for extinction and recurrence of epidemics: estimation and inference for measles outbreaks. Biostatistics 3:493–510.

Fuller, W. A. 1976. Introduction to statistical time series. Wiley, New York.

Glass, K., Y. Xia, and B. T. Grenfell. 2003. Interpreting time-series analysis for continuous-time biological models: measles as a case study. Journal of Theoretical Biology 223:19–25.

Grenfell, B. T., and J. Harwood. 1997. (Meta)population dynamics of infectious diseases. Trends in Ecology & Evolution 12:395–399.

Grenfell, B. T., O. N. Bjørnstad, and J. Kappey. 2001. Travelling waves and spatial hierarchies in measles epidemics. Nature 414:716–723.

Grenfell, B. T., O. N. Bjørnstad, and B. F. Finkenstädt. 2002. Dynamics of measles epidemics: scaling noise, determinism and predictability with the time series SIR model. Ecological Monographs 72:185–202.

Hannan, E. J. 1973. The asymptotic theory of linear time series models. Journal of Applied Probability 10:130–145.

Hanski, I. 1998. Metapopulation dynamics. Nature 396: 41–49.

Hethcote, H. W. 2000. The mathematics of infectious diseases. SIAM Review 42:599–653.

Keeling, M. J., and P. Rohani. 2002. Estimating spatial coupling in epidemiological systems: a mechanistic approach. Ecology Letters 5:20–29.

Keeling, M. J., M. E. J. Woolhouse, R. M. May, G. Davies, and B. T. Grenfell. 2003. Modeling vaccination strategies against foot-and-mouth disease. Nature 421:136–142.

Keeling, M. J., O. N. Bjørnstad, and B. T. Grenfell. 2004. Metapopulation dynamics of infectious diseases. Pages 415–446 *in* I. Hanski and O. Gaggiotti, eds. Ecology, evolution and genetics of metapopulations. Elsevier, Amsterdam.

Kendall, B. E., C. J. Briggs, W. W. Murdoch, P. Turchin,

S. P. Ellner, E. McCauley, R. M. Nisbet, and S. N. Wood. 1999. Inferring the causes of population cycles: a synthesis of statistical and mechanistic modeling approaches. Ecology 80:1789–1805.

Kendall, D. G. 1949. Stochastic processes and population growth. Journal of the Royal Statistical Society B 11: 230–264.

King, A. A., and W. M. Schaffer. 2001. The geometry of a population cycle: a mechanistic model of snowshoe hare demography. Ecology 82:814–830.

Liu, W. M., H. W. Hethcote, and S. A. Levin. 1987. Dynamical behaviour of epidemiological models with nonlinear incidence rates. Journal of Mathematical Biology 25:359–380.

Lloyd, A. L., and R. M. May. 2001. How viruses spread among computers and people. Science 292:1316–1317.

McLean, A. R., and R. M. Anderson. 1988. Measles in developing countries. I. Epidemiological parameters and patterns. Epidemiology and Infection 100:111–133.

Mollison, D. 1995. Epidemic models: their structure and relation to data. Cambridge University Press, Cambridge.

Murdoch, W. W. 1994. Population regulation in theory and practice. Ecology 75:271–287.

Murray, G. D., and A. D. Cliff. 1975. A stochastic model for measles epidemics in a multi-region setting. Institute of British Geographers 2:158–174.

Nåsell, I. 1999. On the time to extinction in recurrent epidemics. Journal of the Royal Statistical Society B 61: 309–330.

Okubo, A. 1980. Diffusion and ecological problem: mathematical models. Springer, Berlin.

Olsen, L. F., and W. M. Schaffer. 1990. Chaos versus noisy periodicity: alternative hypotheses for childhood epidemics. Science 249:499–504.

Priestley, M. B. 1981. Spectral analysis and time series. Academic Press, London.

Rand, D. A., and H. B. Wilson. 1991. Chaotic stochasticity: a ubiquitous source of unpredictability in epidemics. Proceedings of the Royal Society of London B 246:179–184.

Read, J. M., and M. J. Keeling. 2003. Disease evolution on networks: the role of contact structure. Proceedings of the Royal Society of London B 270:699–708.

Rohani, P., M. J. Keeling, and B. T. Grenfell. 2002. The interplay between determinism and stochasticity in childhood diseases. American Naturalist 159:469–481.

Sattenspiel, L., and C. Powell. 1993. Geographic spread of measles on the island of Dominica, West-Indies. Human Biology 65:107–129.

Schenzle, D. 1984. An age-structured model of pre- and post-vaccination measles transmission. IMA Journal of Mathematics Applied in Medicine and Biology 1:169–191.

Schneider, D. W., C. D. Ellis, and K. S. Cummings. 1998. A transportation model assessment of the risk to native mussel communities from zebra mussel spread. Conservation Biology 12:788–800.

Smith, D. L., B. Lucey, L. A. Waller, J. E. Childs, and L. A. Real. 2002. Predicting the spatial dynamics of rabies epidemics on heterogeneous landscapes. Proceedings of the National Academy of Sciences of the USA 99:3668–3672.

Swinton, J. 1998. Extinction times and phase transitions for spatially structured closed epidemics. Bulletin of Mathematical Biology 60:215–230.

Swinton, J., J. Harwood, B. T. Grenfell, and C. A. Gilligan. 1998. Persistence thresholds for phocine distemper virus infection in harbour seal *Phoca vitulina* metapopulations. Journal of Animal Ecology 67:54–68.

Thomas, R. 1999. Reproduction rates in multiregion modeling systems for HIV/AIDS. Journal of Regional Science 39:359–385.

Tilman, D., and P. Kareiva, eds. 1997. Spatial ecology: the role of space in population dynamics and interspecific interactions. Princeton University Press, Princeton, N.J.

Tong, H. 1990. Non-linear time series: a dynamical system approach. Clarendon, Oxford.

Whitcher, B., P. Guttorp, and D. B. Percival. 2000. Wavelet analysis of covariance with application to atmospheric time series. Journal of Geophysical Research 105:14941–14962.

Wilson, H. B., and M. P. Hassell. 1997. Host-parasitoid spatial models: the interplay of demographic stochasticity and dynamics. Proceedings of the Royal Society of London B 264:1189–1195.

Wood, S. N., and M. B. Thomas. 1996. Space, time and persistence of virulent pathogens. Proceedings of the Royal Society of London B 263:673–680.

Associate Editor: Donald L. DeAngelis